ELSEVIER

The formation of Lewis acid/base stabilised phosphanyltrielanes – A theoretical and experimental study

Ulf Vogel [a], Alexey Y. Timoshkin [b], Karl-Christian Schwan [a],
Michael Bodensteiner [a], Manfred Scheer [a,*]

[a] *Institut für Anorganische Chemie, Universität Regensburg, Universitätsstraße 31, 93053 Regensburg, Germany*
[b] *St. Petersburg State University, Department of Chemistry, University pr. 26, 198504 Old Peterhoff, St. Petersburg, Russia*

Abstract

Theoretical investigations on the thermochemistry and the reaction mechanism of the formation of Lewis acid/base stabilised phosphanyltrielanes $D \cdot H_2EPH_2 \cdot A$ (D = Lewis base, A = Lewis acid) were conducted. The reactions of $EH_3 \cdot D$ with $A \cdot PH_3$ to form $D \cdot H_2EPH_2 \cdot A$ and H_2 (E = B, Al, Ga; D = NH_3; A = BH_3, $Cr(CO)_5$) are all exothermic, regardless of whether donors and acceptors are present or absent. The lithium chloride elimination reactions between $EH_2Cl \cdot D$ and $A \cdot PH_2Li$ to give $D \cdot H_2EPH_2 \cdot A$ and LiCl are endothermic for donor/acceptor stabilised compounds, if formation of gaseous LiCl is considered. If solid lithium chloride is considered all reactions are strongly exothermic. Studies of the transition state for H_2-elimination reactions between $EH_3 \cdot D$ and $A \cdot PH_3$ to yield $D \cdot H_2EPH_2 \cdot A$ and H_2 were only successful for E = Al, Ga. In these cases the reaction proceeds via a transition state featuring a five or six-coordinate group 13 element. Different donor molecules do not influence the activation energy of such H_2-elimination reactions, but nevertheless they have an effect on the reaction energy. The synthesis of the $Cr(CO)_5$ substituted phosphanyltrielanes $[(CO)_5Cr(H_2PBH_2 \cdot NMe_3)]$ (3a) and $[(CO)_5Cr(H_2PAlH_2 \cdot NMe_3)]$ (3b), as well as of the dinuclear complex $[(CO)_8Cr_2(\mu-HPBH_2 \cdot NMe_3)_2]$ (4) are described, the latter as a subsequent reaction product of the photolysis of 3a. All compounds were characterised spectroscopically and by X-ray structure analysis.
© 2006 Elsevier B.V. All rights reserved.

Keywords: DFT calculations; Mechanism; Group 13/15 compounds; X-ray structure analysis

1. Introduction

Group 13/15 compounds have been examined thoroughly in the last decades, but mostly the focus in this field was drawn towards compounds bearing organic substituents at the main group elements. Only recently have hydrogen substituted group 13/15 compounds drawn considerable attention. For example phosphine borane adducts of the formula $RPH_2 \cdot BH_3$ (R = H, aryl, alkyl) can act as substrates in dehydrocoupling B–P bond formation reactions catalysed by transition metals or main group Lewis acids. This approach was used for the synthesis of novel phosphanylborane oligomers and polymers $(RPHBH_2)_n$ or $(H_2PBH_2)_n$ [1]. Our group has recently succeeded in the stabilisation of the previously unknown parent compounds of phosphanylboranes, -alanes and -gallanes H_2EPH_2 (E = B, Al, Ga) by stabilising these compounds via coordination of a Lewis base and a Lewis acid to the group 13 element and the phosphorus atom, respectively [2,3]. Thus, the phosphanylalane and -gallane adducts $[(CO)_5W(H_2PEH_2 \cdot NMe_3)]$ (E = Al, Ga) could be synthesized by a H_2 elimination reaction starting from $Me_3N \cdot EH_3$ and $[H_3PW(CO)_5]$ [3]. This approach was not successful in the synthesis of the Lewis acid/base stabilised phosphanylborane $[(CO)_5W(H_2PBH_2 \cdot NMe_3)]$. Instead a reaction sequence incorporating a LiCl elimina-

tion step was necessary to synthesise this compound [2]. Preliminary investigations on the thermochemistry of the H_2 elimination reactions between $Me_3N \cdot EH_3$ and $[H_3PW(CO)_5]$ (E = B, Al, Ga) showed that the reaction is generally exothermic, though to a lesser extent for E = B. In the case of boron the elevated temperatures needed for the synthesis render the Gibbs energy endergonic. For an explanation of these facts an in depth study of the reaction mechanism is needed. In this paper, we present the results of our comprehensive theoretical investigation concerning the thermochemistry and reaction mechanism of the two different approaches used for the synthesis of Lewis acid/base stabilised phosphanyltrielanes. Furthermore, the synthesis and characterisation of $Cr(CO)_5$ substituted phosphanylborane and -alane complexes is presented.

2. Experimental

2.1. Computational details

Density functional theory in the form of the hybrid B3LYP [4] functional was used together with the standard full-electron 6-31G* basis set. For Cr the ECP basis set of Hay and Wadt was used [5]. The GAUSSIAN-98 [6] program suite was used throughout. All structures were fully optimized and verified with subsequent vibrational analysis to be minima or first-order saddle points on the potential energy surface.

2.2. General remarks

All manipulations were performed under an atmosphere of argon or nitrogen in a glovebox or by using standard Schlenk techniques. Solvents were dried by standard procedures and distilled prior to use. NMR Spectra were recorded on a Bruker Avance 400 (400.13 MHz for ^1H, 192.55 MHz for ^{11}B and 161.98 MHz for ^{31}P) and the chemical shifts are referenced to external standards (^1H: $SiMe_4$, ^{11}B: $BF_3 \cdot Et_2O$, ^{31}P: 85% H_3PO_4). Starting materials were synthesized using published procedures: $P(SiMe_3)_3$ [7], $BClH_2 \cdot NMe_3$ [8], $AlH_3 \cdot NMe_3$ [9]. $[Cr(CO)_6]$ was obtained commercially and used as received.

2.3. Preparations

2.3.1. $[(CO)_5Cr(PH_3)]$ (1)

A solution of $[Cr(CO)_6]$ (7.00 g, 31.8 mmol) in 300 ml THF was irradiated by UV-light in a photochemical reactor for ca. 8 h. The completeness of the formation of $[(CO)_5Cr(THF)]$ was monitored by IR-spectroscopy by the disappearance of the absorption for $[Cr(CO)_6]$ ($\tilde{v} = 1979$ cm^{-1}) and the appearance of the absorptions for $[(CO)_5Cr(THF)]$ ($\tilde{v} = 2073$, 1935, 1895 cm^{-1}). The resulting deep-orange solution was transferred into a 500 ml flask and $P(SiMe_3)_3$ (8.77 g, 35 mmol) was added at 0 °C. After stirring for 3 h methanol (4.6 ml, 114 mmol) was added at 0 °C and stirring was continued for an addi-

tional 17 h at room temperature. All volatiles were removed in vacuo and the resulting solid was purified by sublimation (60 °C, 10^{-3} mbar). $[(CO)_5Cr(PH_3)]$ (1) is obtained as a light yellow, crystalline solid (6.70 g, 93%). Anal. Calc. for $C_5H_3O_5P$ (226.04): C, 26.57; H, 1.34. Found: C, 26.68; H, 1.36%. MS (EI, 70 eV) m/z: 225.9 (100) $[M^+]$, 197.9 (8) $[M^+-CO]$, 169.9 (6) $[M^+-2CO]$, 142.0 (8) $[M^+-3CO]$, 113.9 (62) $[M^+-4CO]$, 86.0 (77) $[M^+-5CO]$, 52.0 (68) $[Cr^+]$. IR (CH_2Cl_2): $\tilde{v} = 2356$ (w, PH), 2073 (m, CO), 1980 (sh, CO), 1948 (vs, CO) cm^{-1}. ^1H NMR (C_6D_6): $\delta = 2.32$ (d, $J(P,H) = 332$ Hz, 3H, PH_3). ^{31}P NMR (C_6D_6): $\delta = -129.9$ (q, $J(H,P) = 332$ Hz).

2.3.2. $Li[(H_2P)Cr(CO)_5]$ (2)

To a solution of 1 (6.64 g, 29.4 mmol) in 150 ml of toluene was added a 1.6 M solution of n-BuLi in hexanes (18.4 ml, 29.4 mmol) at 0 °C during 1 h. After stirring for an additional hour at 0 °C the resulting light brown solid was isolated by filtration, washed with toluene (25 ml) and n-pentane (3 × 25 ml) and dried in vacuo to yield $Li[(H_2P)Cr(CO)_5]$ as a light brown, pyrophoric powder (6.60 g, 97%). Due to the pyrophoric nature of the product an elemental analysis could not be determined. ^1H NMR (THF-d_8): $\delta = -0.21$ (d, $J(P,H) = 150$ Hz, 2H, PH_2). ^{31}P NMR (THF-d_8): $\delta = -227.1$ (t, $J(H,P) = 150$ Hz).

2.3.3. $[(CO)_5Cr(H_2PBH_2 \cdot NMe_3)]$ (3a)

To a suspension of 2 (6.60 g, 28.4 mmol) in 75 ml of toluene was added a solution of $BClH_2 \cdot NMe_3$ (2.74 g, 25.5 mmol) in 15 ml of toluene. After stirring at room temperature for 18 h the solution was filtered through a plug of celite (2 × 2.5 cm) and concentrated to ca. 5 ml. Addition of n-hexane (100 ml) precipitated the product, which was isolated by filtration, washed with n-hexane (2 × 25 ml) and dried in vacuo. Compound 3a is obtained as a light yellow powder. A second crop of product can be obtained by concentrating the combined washings and storage at −25 °C (combined yield: 6.50 g, 86% based on $BClH_2 \cdot NMe_3$). Anal. Calc. for $C_8H_{11}BCrNO_5P$ (296.97): C, 32.35; H, 4.41; N, 4.72. Found: C, 32.34; H, 4.52; N, 4.70%. MS (FD) m/z: 296.9 $[M^+]$. IR (CH_2Cl_2): $\tilde{v} = 2425$ (w, BH), 2320 (w, PH), 2059 (m, CO), 1975 (sh, CO), 1931 (vs, CO) cm^{-1}. ^1H NMR (C_6D_6): $\delta = 1.47$ (s, 9H, Me), 2.24 (dm, $J(P,H) = 290$ Hz, 2H, PH_2). ^{11}B NMR (C_6D_6): $\delta = -8.5$ (s, br). ^{31}P NMR (C_6D_6): $\delta = -136.3$ (t, br, $J(H,P) = 290$ Hz).

2.3.4. $[(CO)_5Cr(H_2PAlH_2 \cdot NMe_3)]$ (3b)

To a solution of 1 (448 mg, 1.98 mmol) in 50 ml of n-hexane was added solid $AlH_3 \cdot NMe_3$ (178 mg, 2.00 mmol) and the mixture stirred for 18 h at room temperature. To ensure complete reaction the mixture was heated at reflux for 30 min and filtered while still hot. Slight yellow crystals of 3b (240 mg, 38%) are obtained upon storage of the filtrate at −25 °C. The compound shows decomposition upon storage at room temperature and should thus be kept

at $-78\,°C$. IR (KBr): $\tilde{v} = 2319$ (m, PH), 2060 (s, CO), 1920 (br, vs, CO), 1815 (m, AlH), 1680 (sh, AlH) cm^{-1}. ^{1}H NMR ($CD_2Cl_2/-40\,°C$): $\delta = 1.73$ (d, $J(P,H) = 279$ Hz, 2H, PH_2), 2.59 (s, 9H, NMe_3), 5.70 (s, br, 2H, AlH_2). ^{31}P NMR ($CD_2Cl_2/-40\,°C$): $\delta = -200.7$ (t, br, $J(H,P) = 279$ Hz).

2.3.5. $[(CO)_8Cr_2(\mu\text{-}HPBH_2 \cdot NMe_3)_2]$ (4)

A solution of **3a** (247 mg, 0.83 mmol) in 50 ml of toluene was irradiated by UV light for 18 h. Removal of all volatiles in vacuum left the crude product as a brown solid. Recrystallisation from a minimum amount of CH_2Cl_2 yielded **4** (46 mg, 20%) as red crystals. MS (EI, 70 eV) m/z: 535.9 (12) $[M^+]$, 479.9 (6) $[M^+ - 2CO]$, 452.0 (8) $[M^+ - 3CO]$, 424.0 (36) $[M^+ - 4CO]$, 396.0 (18) $[M^+ - 5CO]$, 340.0 (44) $[M^+ - 7CO]$, 311.9 (100) $[M^+ - 8CO]$. IR (CH_2Cl_2): $\tilde{v} = 2387$ (w, BH), 2305 (m, PH), 2001 (s, CO), 1944 (vs, CO), 1922 (sh, CO) cm^{-1}. ^{1}H NMR (C_6D_6): $\delta = 2.09$ (s, 18H, Me), 5.98 (dt, $J(P,H) = 271$, 6 Hz, 2H, PH). ^{31}P NMR (C_6D_6): $\delta = 196.1$ (d, br, $J(H,P) = 271$ Hz).
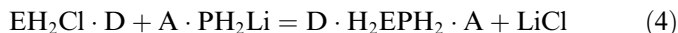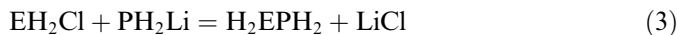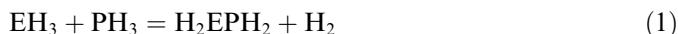
2.4. X-ray structure determinations

Single crystals were obtained from toluene (**3a**), hexane (**3b**) or CH_2Cl_2 (**4**). Data were collected on a STOE IPDS diffractometer using Mo Kα radiation ($\lambda = 0.71073$ Å) for complexes **3a,b** or Ag Kα radiation ($\lambda = 0.56087$ Å) for **4**. The structures were solved by direct methods with the program SHELXS-97 [10a], and full-matrix least-squares refinement on F^2 in SHELXL-97 [10b] was performed with anisotropic displacements for non-H atoms. Hydrogen atoms at carbon atoms were located in idealised positions and refined isotropically according to the riding model. The hydrogen atoms at the phosphorus, aluminium and boron atoms were found as residue electron densities and freely refined.

3. Results and discussion

3.1. Theoretical investigations on the thermochemistry of the formation of phosphanyltrielane complexes

In order to answer the question of what the difference is between the reaction of $D \cdot EH_3$ (D = Lewis base) and $A \cdot PH_3$ (A = Lewis acid) in the case of E = B, where a H_2 elimination reaction is not observed experimentally, and the case of E = Al, Ga, where a H_2 elimination under B–E bond formation is observed, we calculated the thermochemical data on these reactions for different donor and acceptor molecules as well as for the uncoordinated starting materials (Eqs. (1) and (2), A = BH_3, $Cr(CO)_5$; D = NH_3). To consider a second group of reactions we have calculated thermochemical data for a salt elimination reaction between $D \cdot EH_2Cl$ and $A \cdot PH_2Li$ (Eqs. (3) and (4), A = BH_3, $Cr(CO)_5$; D = NH_3).

$$EH_3 + PH_3 = H_2EPH_2 + H_2 \tag{1}$$

$$EH_3 \cdot D + A \cdot PH_3 = D \cdot H_2EPH_2 \cdot A + H_2 \tag{2}$$

$$EH_2Cl + PH_2Li = H_2EPH_2 + LiCl \tag{3}$$

$$EH_2Cl \cdot D + A \cdot PH_2Li = D \cdot H_2EPH_2 \cdot A + LiCl \tag{4}$$

Computed values of the reaction enthalpies, entropies and the Gibbs energies are given in Table 1. It can be seen, that for the elimination of H_2, Gibbs energies for both unstabilised and donor/acceptor stabilized cases are negative and very similar in value, although when E = B the absolute values are noticeably lower than for aluminium and gallium. Thus, elimination of H_2 is thermodynamically allowed and is not affected by the presence of donor and acceptor molecules. In the case of LiCl elimination, there is a noticeable difference between the Gibbs energies for the unstabilised and the donor/acceptor stabilised cases. If gaseous LiCl is considered, LiCl elimination in the Lewis acid/base stabilised case is unfavourable thermodynamically.

Since in the experiment solid LiCl is formed, the process of formation of solid LiCl was considered by taking into account the experimental values of the sublimation energetics of LiCl (sublimation enthalpy 213.1 kJ mol^{-1} and sublimation entropy 153.5 J mol^{-1} K^{-1} [11]). Formation of solid LiCl is clearly favourable thermodynamically both for the unstabilised and donor/acceptor stabilised cases.

As a result of this investigation it can be concluded, that the answer to the question of why the Lewis acid/base stabilised phosphanylborane complexes cannot be synthesized by a H_2 elimination reaction cannot be found in the thermodynamics of the reaction. To gain further insight into the mechanism of the H_2 elimination reaction, computations on the transition state of the reaction have been performed.

3.2. Role of the donor centre in the transition state

In order to understand the influence of the donor centre on the H_2 elimination reactions, optimisation of the transition state (TS) has been performed for the selected donor molecules. Such optimisation was successful only for Al- and Ga-containing compounds; we were not able to locate transition states for the boron containing molecules. Results obtained for the Al and Ga compounds are given in Table 2. In the case of NH_3 as a donor molecule, the intrinsic reaction coordinate scan (IRC) has been performed to confirm that the obtained transition state connects the source molecules $NH_3 \cdot AlH_3 + PH_3 \cdot BH_3$ and the products $NH_3 \cdot AlH_2PH_2 \cdot BH_3 + H_2$. The optimised structure of the TS for this case, as well as the structures for the IRC scan in the backward and forward directions are presented in Fig. 1. The optimised structure of the TS for the formation of $NMe_3 \cdot AlH_2PH_2Cr(CO)_5$ (Fig. 2) has similar structural and energetic parameters. In fact, for the reaction $NH_3 \cdot AlH_3 + PH_3 \cdot BH_3 = NH_3 \cdot AlH_2$-$PH_2 \cdot BH_3 + H_2$ the reaction barrier is 139.8 kJ mol^{-1}

Table 1
Calculated thermodynamic characteristics of H_2 and LiCl elimination reactions, B3LYP/6-31G* level of theory

Process	ΔH^0_{298}	ΔS^0_{298}	ΔG^0_{298}	ΔG^0_{398}
$BH_3 + PH_3 = H_2BPH_2 + H_2$	−17.0	−13.7	−12.9	−11.5
$AlH_3 + PH_3 = H_2AlPH_2 + H_2$	−28.8	−7.6	−26.5	−25.8
$GaH_3 + PH_3 = H_2GaPH_2 + H_2$	−31.9	−9.0	−29.2	−28.3
$NH_3 \cdot BH_3 + PH_3 \cdot BH_3 = NH_3H_2BPH_2 \cdot BH_3 + H_2$	−21.9	−31.9	−12.3	−9.1
$NH_3 \cdot AlH_3 + PH_3 \cdot BH_3 = NH_3 \cdot H_2AlPH_2 \cdot BH_3 + H_2$	−32.2	−8.2	−29.7	−28.9
$NH_3 \cdot GaH_3 + PH_3 \cdot BH_3 = NH_3 \cdot H_2GaPH_2 \cdot BH_3 + H_2$	−31.6	−9.8	−28.7	−27.7
$BH_2Cl + PH_2Li = H_2BPH_2 + LiCl$ (gas)	−92.9	−17.1	−87.8	−86.1
$BH_2Cl + PH_2Li = H_2BPH_2 + LiCl$ (solid)	−306.1	−170.6	−255.2	−238.1
$AlH_2Cl + PH_2Li = H_2AlPH_2 + LiCl$ (gas)	−46.6	−10.9	−43.4	−42.3
$AlH_2Cl + PH_2Li = H_2AlPH_2 + LiCl$ (solid)	−259.8	−164.3	−210.8	−194.3
$GaH_2Cl + PH_2Li = H_2GaPH_2 + LiCl$ (gas)	−83.9	−13.2	−79.9	−78.6
$GaH_2Cl + PH_2Li = H_2GaPH_2 + LiCl$ (solid)	−297.0	−166.6	−247.3	−230.7
$NH_3 \cdot BH_2Cl + PH_2Li \cdot BH_3 = NH_3 \cdot H_2BPH_2 \cdot BH_3 + LiCl$ (gas)	3.0	−4.0	4.2	4.6
$NH_3 \cdot BH_2Cl + PH_2Li \cdot BH_3 = NH_3 \cdot H_2BPH_2 \cdot BH_3 + LiCl$ (solid)	−210.2	−157.4	−163.2	−147.5
$NH_3 \cdot AlH_2Cl + PH_2Li \cdot BH_3 = NH_3 \cdot H_2AlPH_2 \cdot BH_3 + LiCl$ (gas)	68.4	7.4	66.2	65.5
$NH_3 \cdot AlH_2Cl + PH_2Li \cdot BH_3 = NH_3 \cdot H_2AlPH_2 \cdot BH_3 + LiCl$ (solid)	−144.7	−146.0	−101.2	−86.6
$NH_3 \cdot GaH_2Cl + PH_2Li \cdot BH_3 = NH_3 \cdot H_2GaPH_2 \cdot BH_3 + LiCl$ (gas)	35.0	1.9	34.4	34.2
$NH_3 \cdot GaH_2Cl + PH_2Li \cdot BH_3 = NH_3 \cdot H_2GaPH_2 \cdot BH_3 + LiCl$ (solid)	−178.2	−151.6	−133.0	−117.8
$NH_3 \cdot BH_3 + PH_3Cr(CO)_5 = NH_3 \cdot H_2BPH_2Cr(CO)_5 + H_2$	−25.8	−57.5	−8.6	−2.9
$NH_3 \cdot BH_2Cl + PH_2LiCr(CO)_5 = NH_3 \cdot H_2BPH_2Cr(CO)_5 + LiCl$ (gas)	−25.0	−10.5	−21.9	−20.8
$NH_3 \cdot BH_2Cl + PH_2LiCr(CO)_5 = NH_3 \cdot H_2BPH_2Cr(CO)_5 + LiCl$ (solid)	−238.1	−164.0	−189.2	−172.8
$NH_3 \cdot AlH_3 + PH_3Cr(CO)_5 = NH_3 \cdot H_2AlPH_2Cr(CO)_5 + H_2$	−31.6	−37.3	−20.4	−16.7
$NH_3 \cdot AlH_2Cl + PH_2LiCr(CO)_5 = NH_3 \cdot H_2AlPH_2Cr(CO)_5 + LiCl$ (gas)	45.0	−2.7	45.8	46.1
$NH_3 \cdot AlH_2Cl + PH_2LiCr(CO)_5 = NH_3 \cdot H_2AlPH_2Cr(CO)_5 + LiCl$ (solid)	−168.1	−156.1	−121.6	−105.9
$NH_3 \cdot GaH_3 + PH_3Cr(CO)_5 = NH_3 \cdot H_2GaPH_2Cr(CO)_5 + H_2$	−32.5	−38.8	−21.0	−17.1
$NH_3 \cdot GaH_2Cl + PH_2LiCr(CO)_5 = NH_3 \cdot H_2GaPH_2Cr(CO)_5 + LiCl$ (gas)	10.0	−8.0	12.4	13.2
$NH_3 \cdot GaH_2Cl + PH_2LiCr(CO)_5 = NH_3 \cdot H_2GaPH_2Cr(CO)_5 + LiCl$ (solid)	−203.1	−161.5	−155.0	−138.8

Data for the reactions for solid LiCl are calculated using experimental values of sublimation enthalpy (213.1 kJ mol^{-1}) and sublimation entropy (153.5 J mol^{-1} K^{-1}) [11] (values for ΔH^0 and ΔG^0 in kJ mol^{-1}, for ΔS^0 in J mol^{-1} K^{-1}).

Table 2
Bond dissociation energies of $D \cdot EH_3$ and activation and reaction energies E_0 (kJ mol^{-1}) for the H_2 elimination from the donor/acceptor stabilised compounds: $D \cdot EH_3 + PH_3 \cdot BH_3 = D \cdot EH_2PH_2 \cdot BH_3 + H_2$

Donor molecule D	$D \cdot EH_3 = EH_3 + D$			$D \cdot EH_3 + PH_3 \cdot BH_3 = H_2 + D \cdot EH_2–PH_2 \cdot BH_3$			
	E = B	E = Al	E = Ga	TS energy		Reaction energy	
				E = Al	E = Ga	E = Al	E = Ga
NH_3	137.8	134.7	113.8	140.6	172.4	−27.7	−26.8
NMe_3	144.1	127.5	108.9	139.8	169.5	−27.1	−26.7
py	139.8	125.4	105.4	132.0	163.1	−53.4	−49.6
dmap	151.9	142.5	[a]	124.5	[a]	−42.6	[a]
Carbene	[a]	192.9	179.9	137.0	171.8	−12.3	[a]
Me-carbene	246.4	198.6	185.0	137.3	[a]	[a]	[a]

B3LYP/6-31G* level of theory (py = pyridine, dmap = 4-(dimethylamino)pyridine, carbene = imidazol-2-ylidene, Me-carbene = tetramethylimidazol-2-ylidene).
[a] Value not computed.

and the reaction energy −27.1 kJ mol^{-1}, while for the reaction $NMe_3 \cdot AlH_3 + PH_3Cr(CO)_5 = NMe_3 \cdot AlH_2PH_2$-$Cr(CO)_5 + H_2$ the activation energy is 131.0 kJ mol^{-1} and the reaction energy −38 kJ mol^{-1}.

The energy of the transition state does not show significant variation for the various donor molecules in the cases of E = Al and Ga which allows the conclusion that the H_2 elimination reaction between $D \cdot EH_3$ and $A \cdot PH_3$ should take place with a broad variation of different donor molecules – a fact that has also been observed in different experiments [12]. While the donor molecule does not seem to influence the energy of the transition state, it has a definitive influence on the reaction energy, albeit not a very strong one. Reactions of amine stabilised trielanes are less exothermic than reactions with a pyridine unit as a Lewis base. When N-heterocyclic carbenes are used as a Lewis
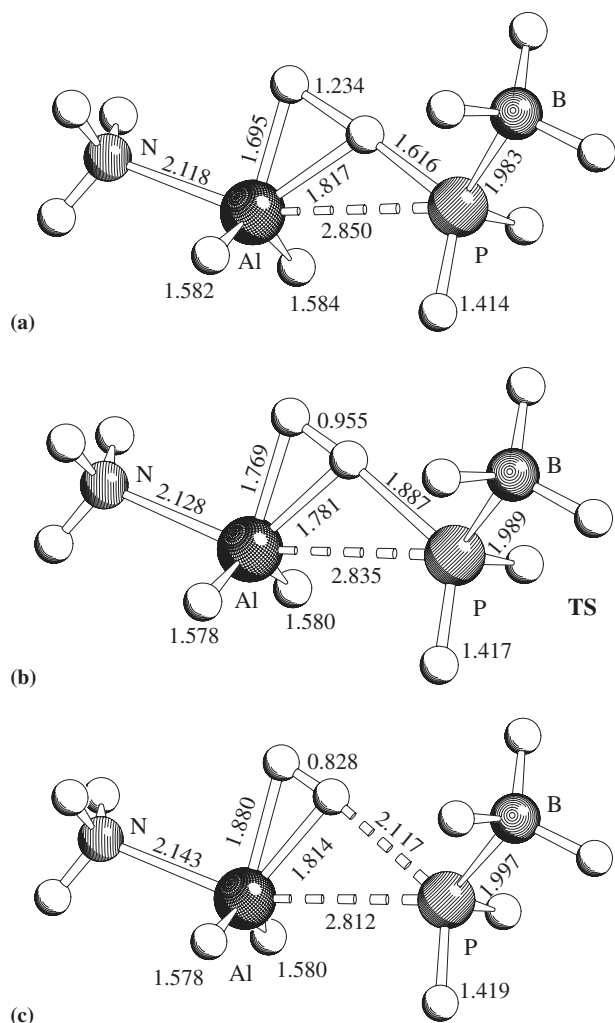
Fig. 1. Optimised geometry of the transition state for the intermolecular H$_2$ elimination (b) and structures on the intrinsic reaction path in the forward (c) and backward (a) directions (interatomic distances are given in Å).
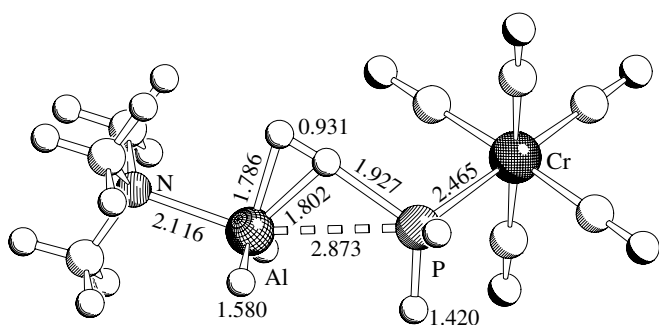

Fig. 2. Structure of the TS for the reaction NMe$_3$AlH$_3$ + PH$_3$Cr-(CO)$_5$ = NMe$_3$AlH$_2$PH$_2$Cr(CO)$_5$ + H$_2$ (interatomic distances are given in Å).

base the reaction energy decreases in comparison with simple amines, but still remains exothermic.

To conclude, it can be said that the H$_2$ elimination reaction seems to proceed via a transition state where the aluminium or gallium atom shows a coordination number of five (or six if the long P–Al distance of ca. 285 pm is taken into account). For aluminium and gallium this coordination number is not uncommon and is observed in the structures of a variety of compounds. Boron, however, prefers a coordination number of four or less. This might be an explanation why we could not locate a transition state for the H$_2$ elimination reactions featuring boron containing compounds. The nature of the donor molecule does not influence the transition state energy for Al and Ga, but it has an impact on the reaction energy.

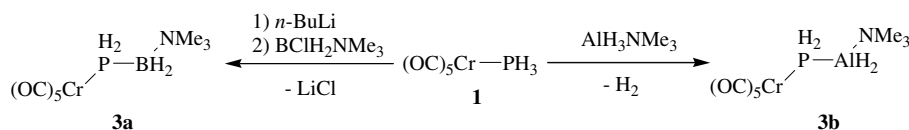### 3.3. Synthesis and spectroscopic characterisation of the complexes

The synthesis of [(CO)$_5$Cr(PH$_3$)] (**1**) can be achieved in high yields by a methodology analogous to the synthesis of [(CO)$_5$W(PH$_3$)] [13] avoiding the use of gaseous PH$_3$. According to Scheme 1 [Cr(CO)$_6$] is converted to [(CO)$_5$Cr(THF)] by photolysis in tetrahydrofuran. Addition of P(SiMe$_3$)$_3$ and subsequent alcoholysis with methanol yields **1** in 93% yield after sublimation.

Complex **1** can be converted to the phosphanylborane complex [(CO)$_5$Cr(H$_2$PBH$_2$ · NMe$_3$)] (**3a**) by a salt elimination reaction. Lithiation of **1** with *n*-BuLi and reaction of the resulting Li[(H$_2$P)Cr(CO)$_5$] (**2**) with BClH$_2$ · NMe$_3$ gives **3a** in high yield. The corresponding phosphanylalane complex [(CO)$_5$Cr(H$_2$PAlH$_2$ · NMe$_3$)] (**3b**) is synthesised by a H$_2$-elimination reaction between **1** and AlH$_3$ · NMe$_3$ in *n*-hexane (Scheme 2). The product **3b** can be isolated in moderate yields by crystallisation from the filtered reaction mixture. Both compounds have been characterised spectroscopically and by single crystal X-ray structure analysis.

Complex **3a** is a light yellow solid which is sparingly soluble in *n*-hexane and readily soluble in toluene or dichloromethane. The IR spectrum of **3a** shows a prominent peak for a BH valence vibration at 2425 cm^{-1}, as well as an absorption due to the PH stretching at 2320 cm^{-1}. In the region of terminal CO ligands, three absorptions are detected as is expected for the Cr(CO)$_5$ moiety with its local C_{4v} symmetry. Compound **3a** shows a triplet in the ^{31}P NMR spectrum at −136.3 ppm with a ^1J(H, P) coupling constant of 290 Hz which is typical for tetracoordinated phosphorus. The signal is significantly broadened due to the quadrupole moment of the $^{10/11}$B nuclei directly attached to the phosphorus atom. This also influences the ^{1}H NMR spectrum in which signals for the BH$_2$ protons

$$(OC)_5Cr-THF \xrightarrow{P(SiMe_3)_3} (OC)_5Cr-P(SiMe_3)_3 \xrightarrow[-\text{MeOSiMe}_3]{\text{MeOH}} (OC)_5Cr-PH_3$$

1
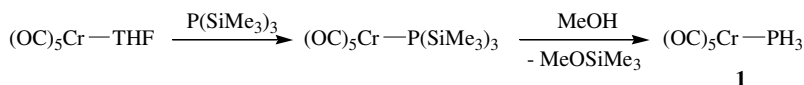
Scheme 1. Synthesis of [(CO)$_5$Cr(PH$_3$)] (**1**).

Scheme 2. Synthesis of [(CO)$_5$Cr(H$_2$PBH$_2$ · NMe$_3$)] (**3a**) and [(CO)$_5$Cr(H$_2$PAlH$_2$ · NMe$_3$)] (**3b**).

cannot be detected, but a singlet for the NMe$_3$ protons and a multiplet for the PH$_2$ protons are found.

Complex **3b** is a light yellow solid sparingly soluble in hydrocarbons. It dissolves well in more polar solvents like toluene or dichloromethane, but shows fast decomposition in these solvents at ambient temperature. The nature of the degradation products could not be determined, but investigations on the decomposition of the tungsten analogue of **3b** in THF reveal the formation of the anionic species [(CO)$_5$W(μ-PH$_2$)W(CO)$_5$]$^-$ [14]. At lower temperatures solutions of **3b** in toluene and dichloromethane are stable for a limited time, which allowed us to record NMR spectra of the compound. The ^{31}P NMR spectrum of **3b** shows a prominent triplet for the PH$_2$ group at −200.7 ppm ($J(H, P) = 279$ Hz). The ^{1}H NMR spectrum of **3b** displays signals for the NMe$_3$ and PH$_2$ groups, as well as a broad signal at 5.70 ppm for the Al–H protons. With the NMR data discussed above no definitive conclusion can be drawn on whether **3b** is associated in solution or monomeric. However, the X-ray structure analysis of **3b** shows dimeric aggregates in the solid state. Additional evidence for this dimerisation can be found in the IR spectrum of **3b** in KBr, which shows a broad band at 1680 cm^{-1} typical of Al–H···Al bridges.

In contrast to the instability of **3b** in solvents other than hexanes, **3a** shows no decomposition reactions in solution. In order to induce H$_2$ elimination, a solution of **3a** in toluene was irradiated with UV light for 18 h, which caused a colour change from light yellow to red. After workup of the reaction mixture the compound [(CO)$_8$Cr$_2$-(μ-HPBH$_2$ · NMe$_3$)$_2$] (**4**) could be isolated (Scheme 3).

Complex **4** is an orange solid which is moderately soluble in toluene and CH$_2$Cl$_2$. In its ^{31}P NMR spectrum it shows a broad doublet at 196.1 ppm with a $J(P, H)$ coupling constant of 271 Hz. In comparison to the starting complex **3a** ($\delta = -136.3$ ppm) the signal is significantly shifted to low field. This feature is commonly observed when a phosphanido ligand bridges a metal–metal bond and therefore changes the bond angles. For example the

signal for [Cp′(CO)$_2$Mn(μ-PH$_2$)Fe(CO)$_2$Cp] at −62 ppm is shifted downfield to 76 ppm when the compound is irradiated with UV light and the complex [Cp′(CO)Mn(μ-PH$_2$)(μ-CO)Fe(CO)Cp] with a metal–metal bond is formed [15]. The ^{1}H NMR spectrum of **4** shows a singlet for the NMe$_3$ protons at 2.09 ppm and a doublet of triplets at 5.98 ppm ($J(H, P) = 271$, 6 Hz) for the protons bound to the phosphorus atoms, due to their coupling with phosphorus and the two protons of the BH$_2$ group. Signals for the protons at the boron atom could not be detected (see discussion above). The IR spectrum of **4** in CH$_2$Cl$_2$ shows an absorption for the BH and PH bond stretching, as well as three bands for the CO bond stretching, indicating that the local D_{2h} symmetry of the cluster core found in the solid state structure is retained in solution.

3.4. X-ray structure determinations

The molecular structures of the compounds **3a**, **3b** and **4** were determined by single crystal X-ray diffraction. The crystal data and the experimental parameters used for the crystal structure analysis are summarised in Table 3. Molecular structures of the compounds are depicted in Figs. 3–5.

Complex **3a** crystallises in the monoclinic space group $P2_1/c$. The parameters of the unit cell are only slightly different to the previously described tungsten derivative [(CO)$_5$W(H$_2$PBH$_2$ · NMe$_3$)] [2]. The key structural feature is a H$_2$PBH$_2$ moiety which is coordinated to a Cr(CO)$_5$ fragment via the lone electron pair at the phosphorus atom. The coordination sphere of the boron atom is completed by the coordination of a NMe$_3$ molecule. The substituents at the B–P bond are arranged in a staggered conformation where the NMe$_3$ and Cr(CO)$_5$ fragments are *trans* to each other (torsion angle Cr–P–B–N 179.54(1)°). The B–P bond length is comparable to that in [(CO)$_5$W(H$_2$PBH$_2$ · NMe$_3$)] (**3a**: 196.4(3) pm, [(CO)$_5$W(H$_2$PBH$_2$ · NMe$_3$)]: 195.5(4) pm [2]). The B–N bond length is in a range usually found for similar compounds (**3a**: 159.9(3) pm, [(CO)$_5$W(H$_2$PBH$_2$ · NMe$_3$)]: 160.3(5) pm [2]). The Cr–P bond length of **3a** displays a comparable value to substituted phosphine complexes of Cr(CO)$_5$ (**3a**: 239.7(1) pm, [(CO)$_5$Cr(PMe$_3$)] 236.64(5) pm [16], [(CO)$_5$Cr(PPh$_3$)] 242.2(1) pm [17]).

Complex **3b** crystallises in the monoclinic space group $P2_1/c$ and is isostructural with the corresponding tungsten derivative [(CO)$_5$W(H$_2$PAlH$_2$ · NMe$_3$)] [3]. The molecular structure displays a H$_2$PAlH$_2$ unit which is coordinating to a Cr(CO)$_5$ fragment with the lone pair at the phosphorus atom. A NMe$_3$ molecule is coordinated to the aluminium atom. Two such moieties form a dimeric unit in the solid

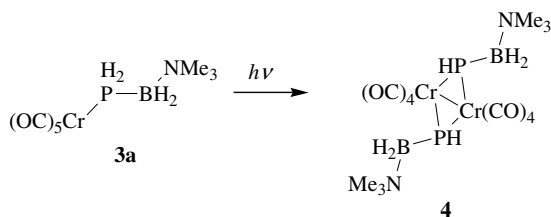Scheme 3. Synthesis of [(CO)$_8$Cr$_2$(μ-HPBH$_2$ · NMe$_3$)$_2$] (**4**) by UV irradiation of **3a**.

Table 3
Crystal data and experimental parameters for the crystal structure determinations of **3a**, **3b** and **4**

Compound	3a	3b	4
Empirical formula	$C_8H_{13}BCrNO_5P$	$C_8H_{13}AlCrNO_5P$	$C_{14}H_{24}B_2Cr_2N_2O_8P_2$
Formula mass (g mol^{-1})	296.97	313.14	535.91
Collection T (K)	200(1)	200(1)	203(2)
λ (Å)	0.71073	0.71073	0.56087
Crystal system	Monoclinic	Monoclinic	Monoclinic
Space group	$P2_1/c$	$P2_1/c$	$P2_1/c$
a (Å)	10.439(2)	6.491(1)	10.368(2)
b (Å)	14.619(3)	13.337(3)	12.696(3)
c (Å)	9.882(2)	17.261(4)	18.466(4)
α (°)	90	90	90
β (°)	108.65(3)	100.55(3)	92.35
γ (°)	90	90	90
V (Å^3)	1428.9(5)	1469.0(5)	2428.7(8)
Z	4	4	4
D_{calc} (g cm^{-1})	1.380	1.416	1.466
μ (mm^{-1})	0.918	0.953	0.555
$F(000)$	608	640	1096
Crystal dimensions (mm)	$0.30 \times 0.15 \times 0.15$	$0.30 \times 0.15 \times 0.15$	$0.15 \times 0.08 \times 0.06$
2θ Range (°)	4.12–48.16	3.88–48.26	3.08–42.00
Index ranges	$-11 \leqslant h \leqslant 11$, $-16 \leqslant k \leqslant 16$, $-11 \leqslant l \leqslant 11$	$-7 \leqslant h \leqslant 6$, $-11 \leqslant k \leqslant 15$, $-19 \leqslant l \leqslant 19$	$-13 \leqslant h \leqslant 9$, $-16 \leqslant k \leqslant 16$, $-22 \leqslant l \leqslant 23$
Reflections collected	6175	5684	12294
Independent reflections	2135	2175	5076
R_{int}	0.0370	0.0272	0.0688
Restraints	–	–	–
Parameters	173	173	301
R_1[a] $[I > 2\sigma(I)]$	0.0326	0.0290	0.0482
wR_2[b] (all data)	0.0857	0.0740	0.1059
Maximum/minimum residual electron density (e Å^{-3})	0.200/−0.220	0.290/−0.229	0.347/−0.344

[a] $R_1 = \sum ||F_o| - |F_c||/\sum |F_o|$.
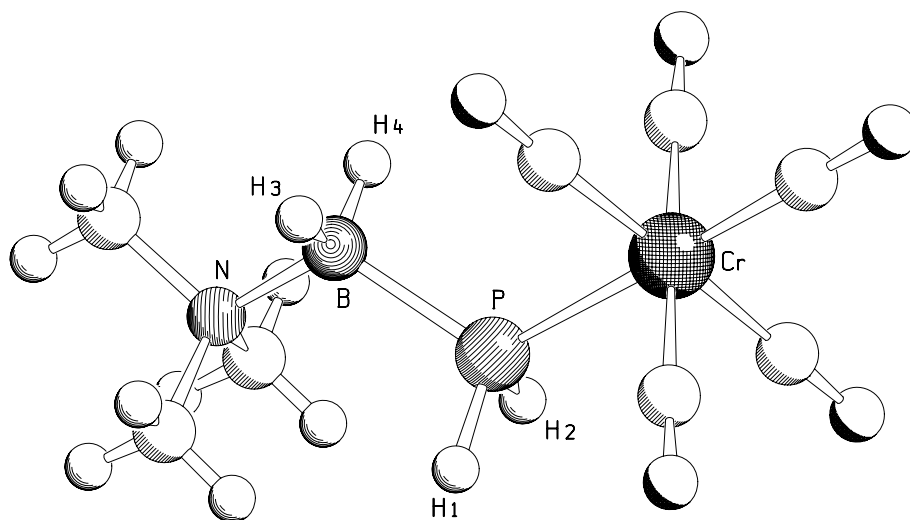[b] $wR_2 = [\sum \omega (F_o^2 - F_c^2)^2]/[\sum (F_o^2)^2]^{1/2}$.

Fig. 3. Molecular structure of **3a** in the crystal. Selected bond lengths (pm) and angles (°): Cr–P, 239.7(1); P–B, 196.4(3); B–N, 159.9(3); Cr–P–B, 117.33(9); P–B–N, 116.3(2).

state by means of hydride bridges between two aluminium atoms. As a consequence of this dimerisation the aluminium atoms show a distorted trigonal bipyramidal coordination environment. The distance between the two aluminium atoms is in the usual range for such species (**3b**:

291.6(1) pm, [(CO)$_5$W(H$_2$PAlH$_2$ · NMe$_3$)] 290.8(2) pm [3], (H$_3$Al · NMe$_2$CH$_2$Ph)$_2$ 288.3(2) pm [18]). This dimerisation was also observed for the tungsten analogue of **3b**. In comparison with [(CO)$_5$W(H$_2$PAlH$_2$ · NMe$_3$)] the Al–P and Al–N bond lengths in **3b** show only minor deviations (**3b**:
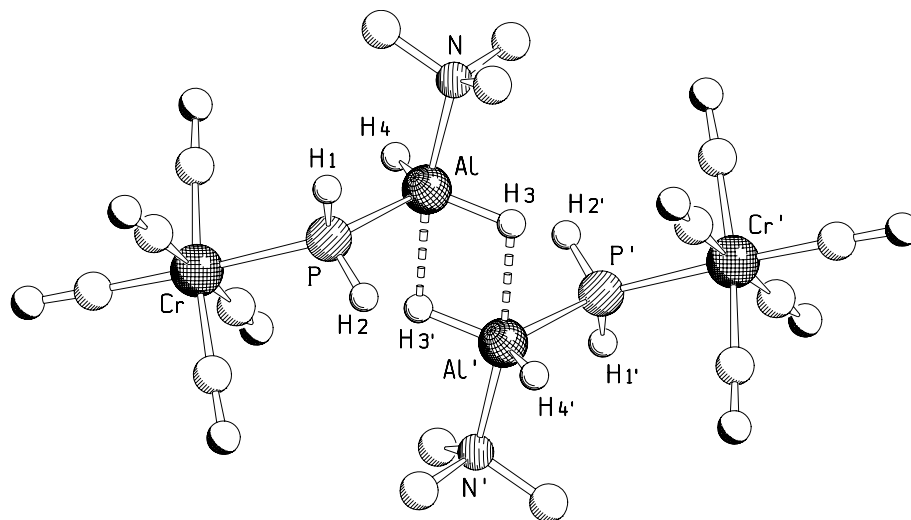
Fig. 4. Molecular structure of **3b** in the crystal (hydrogen atoms on carbon atoms are omitted for clarity). Selected bond lengths (pm) and angles (°): Cr–P, 241.8(1); P–Al, 238.3(1); Al–N, 204.4(2); Al–Al′, 291.6(1); Al–P–Cr, 119.67(4); N–Al–P, 103.16(6); N–Al–Al′, 139.21(6); P–Al–Al′, 95.86(4).
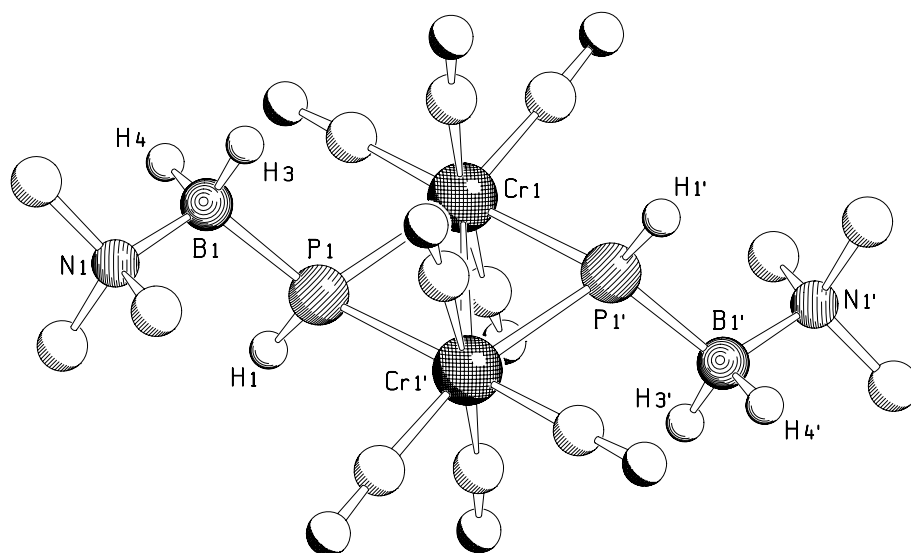

Fig. 5. Molecular structure of **4** in the crystal (hydrogen atoms on carbon atoms omitted for clarity). Only one of the two independent molecules (molecule A) in the asymmetric unit is depicted. Selected bond lengths (pm) and angles (°) (corresponding values for molecule B are given in square brackets): Cr1–P1, 235.7(1) [235.4(1)]; Cr1–P1′, 238.2(1) [237.1(1)]; Cr1–Cr1′, 293.2(1) [292.1(1)]; P1–B1, 197.6(4) [197.6(4)]; B1–N1, 161.9(5) [159.9(5)]; Cr1–P1–Cr1′, 76.44(4) [76.37(4)]; P1–Cr1–P1′, 103.55(4) [103.63(4)]; P1–Cr1–Cr1′, 52.16(3) [52.06(3)]; P1′–Cr1–Cr1′, 51.40(3) [51.57(4)]; B1–P1–Cr1, 130.2(2) [126.5(2)]; B1–P1–Cr1′, 113.2(1) [117.0(2)]; N1–B1–P1, 116.6(3) [116.0(3)].

238.3(1) pm (Al–P), 204.4(2) pm (Al–N); [(CO)₅W(H₂PAl-H₂ · NMe₃)]: 236.7(1) pm (Al–P), 203.6(3) pm (Al–N) [3]). The Cr–P distance in **3b** is comparable with that in **3a** (**3b**: 241.8(1) pm, **3a**: 239.7(1) pm).

Complex **4** crystallises in the monoclinic space group $P2_1/c$ with two independent molecules in the asymmetric unit. Both molecules differ mainly in the conformation of the BH₂ · NMe₃ groups, the bond lengths and angles in the core structure are showing only minor differences. In the following discussion bond lengths and angles for the second molecule are given in square brackets. The key structural feature of **4** is a Cr₂(CO)₈ unit in which the Cr–Cr bond is bridged by two HPBH₂ · NMe₃ moieties in

a way that the BH₂ · NMe₃ fragments are arranged in a *trans* conformation. With 293.2(1) [292.1(1) pm] the Cr–Cr bond length is comparable to corresponding chromium complexes where the metal–metal bond is bridged by two phosphanido ligands ([(CO)₄Cr(μ-PMe₂)₂Cr(CO)₄]: 290.2(1), 290.8(1) pm [19]). The bridging phosphanidoboranyl units are asymmetrically connected to the two chromium atoms, but the difference in the two respective bond lengths is minimal (Cr1–P1 235.7(1) pm [235.4(1) pm]; Cr1–P1′ 238.2(1) pm [237.1(1) pm]). For the structurally comparable complex [(CO)₄Cr(μ-PMe₂)₂Cr(CO)₄] a symmetric bridging mode of the phosphanido ligands is found (Cr–P: 231.8(2) pm [19]). In comparison to the starting

material **3a** the B–P bond is only slightly elongated (**3a**: 196.4(3) pm; **4**: 197.6(4) pm [197.6(4) pm]).

4. Conclusion

We have shown that the reaction of a trielane with phosphine to yield a phosphanyltrielane complex by H_2 elimination is exothermic regardless of whether the starting compounds are stabilised by a Lewis acid/base or not. Complexation of the reactants with Lewis acids and bases has only a negligible influence on the reaction energies. In the case of boron as the group 13 element the reaction energies are still exothermic but to a lesser extent than with aluminium or gallium. Lithium chloride elimination reactions yielding a phosphanyltrielane are strongly influenced by this complexation if the formation of gaseous LiCl is considered. Taking into account that solid LiCl is formed during the reactions renders all reaction energies strongly exothermic.

The transition state of the H_2 elimination reaction was found to contain a five-coordinate aluminium or gallium atom, which could not be calculated for boron even in a different TS arrangement. Thus the strong tendency of gallium and aluminium to be pentacoordinate explains the fact why the H_2 elimination reaction is experimentally observed only for these two elements. In contrast, the preference of boron for tri- or tetracoordination seems to exclude the occurrence of a H_2 elimination reaction. Different Lewis bases do not influence the energy of the transition state, but have an influence on the reaction energies for aluminium and gallium.

Furthermore, we could show that in comparison with $W(CO)_5$ the use of $Cr(CO)_5$ as a Lewis acidic fragment in the formation of the corresponding stabilised phosphanylalanes and -boranes has no detectable influence on the nature of the reaction products and the reactivity pattern of the formed compounds.

5. Supplementary data

Crystallographic data reported in this paper has been deposited with the Cambridge Crystallographic Data Centre as CCDC-296796 (**3a**), -296797 (**3b**) and -296798 (**4**). Copies of the data can be obtained free of charge on application to CCDC, 12 Union Road, Cambridge CB2 1EZ, UK (fax: +44 1223 336 033; e-mail: deposit@ccdc.cam. ac.uk).

Acknowledgements

References

[1] (a) H. Dorn, R.A. Singh, J.A. Massey, A.J. Lough, I. Manners, Angew. Chem., Int. Ed. 38 (1999) 3321–3323;
(b) H. Dorn, R.A. Singh, J.A. Massey, A.J. Lough, I. Manners, Angew. Chem. 111 (1999) 3540–3543;
(c) H. Dorn, R.A. Singh, J.A. Massey, J.M. Nelson, C.A. Jaska, A.J. Lough, I. Manners, J. Am. Chem. Soc. 122 (2000) 6669–6678;
(d) H. Dorn, E. Vejzovic, A.J. Lough, I. Manners, Inorg. Chem. 40 (2001) 4327–4331;
(e) H. Dorn, J.M. Rodezno, B. Brunnhöfer, E. Rivard, J.A. Massey, I. Manners, Macromolecules 36 (2003) 291–297;
(f) J.-M. Denis, H. Forintos, H. Szelke, L. Toupet, T.-N. Pham, P.-J. Madec, A.-C. Gaumont, Chem. Commun. (2003) 54–55.
[2] U. Vogel, P. Hoemensch, K.-C. Schwan, A.Y. Timoshkin, M. Scheer, Chem. Eur. J. 9 (2003) 515–519.
[3] U. Vogel, A.Y. Timoshkin, M. Scheer, Angew. Chem. 113 (2001) 4541–4544;
Angew. Chem., Int. Ed. 40 (2001) 4409–4412.
[4] (a) A.D. Becke, J. Chem. Phys. 98 (1993) 5648–5652;
(b) C. Lee, W. Yang, R.G. Parr, Phys. Rev. B 37 (1988) 785–789.
[5] (a) P.J. Hay, W.R. Wadt, J. Chem. Phys. 82 (1985) 270–283;
(b) W.R. Wadt, P.J. Hay, J. Chem. Phys. 82 (1985) 284–298;
(c) P.J. Hay, W.R. Wadt, J. Chem. Phys. 82 (1985) 299–310.
[6] M.J. Frisch, G.W. Trucks, H.B. Schlegel, G.E. Scuseria, M.A. Robb, J.R. Cheeseman, V.G. Zakrzewski, J.A. Montgomery Jr., R.E. Stratmann, J.C. Burant, S. Dapprich, J.M. Millam, A.D. Daniels, K.N. Kudin, M.C. Strain, O. Farkas, J. Tomasi, V. Barone, M. Cossi, R. Cammi, B. Mennucci, C. Pomelli, C. Adamo, S. Clifford, J. Ochterski, G.A. Petersson, P.Y. Ayala, Q. Cui, K. Morokuma, D.K. Malick, A.D. Rabuck, K. Raghavachari, J.B. Foresman, J. Cioslowski, J.V. Ortiz, B.B. Stefanov, G. Liu, A. Liashenko, P. Piskorz, I. Komaromi, R. Gomperts, R.L. Martin, D.J. Fox, T. Keith, M.A. Al-Laham, C.Y. Peng, A. Nanayakkara, C. Gonzalez, M. Challacombe, P.M.W. Gill, B. Johnson, W. Chen, M.W. Wong, J.L. Andres, C. Gonzalez, M. Head-Gordon, E.S. Replogle, J.A. Pople, GAUSSIAN-98, Revision A.3, Gaussian, Inc., Pittsburgh, PA, 1998.
[7] F. Uhlig, S. Gremler, M. Dargatz, M. Scheer, E. Herrmann, Z. Anorg. Allg. Chem. 606 (1991) 105–108.
[8] G.E. Ryschkewitsch, J.W. Wiggins, Inorg. Synth. 12 (1970) 116–126.
[9] K. Ruff, Inorg. Synth. 9 (1967) 30–37.
[10] (a) G.M. Sheldrick, SHELXS-97, Universität Göttingen, Göttingen, Germany, 1996;
(b) G.M. Sheldrick, SHELXL-97, Universität Göttingen, Göttingen, Germany, 1997.
[11] V.S. Yungman (Ed.), Electronic Database "Thermal Constants of Substances", Version 24.07.2004. Available from: <http://www.chem.msu.su/cgi-bin/tkv.pl?show=welcome.html>.
[12] U. Vogel, K.-C. Schwan, M. Scheer, unpublished results.
[13] U. Vogel, M. Scheer, Z. Anorg. Allg. Chem. 627 (2001) 1593–1598.
[14] U. Vogel, K.-C. Schwan, M. Scheer, Eur. J. Inorg. Chem. (2004) 2062–2065.
[15] H. Schäfer, W. Leske, Z. Anorg. Allg. Chem. 552 (1985) 50–68.
[16] K.J. Lee, T.L. Brown, Inorg. Chem. 31 (1992) 289–294.
[17] H.J. Plastas, J.M. Stewart, S.O. Grim, Inorg. Chem. 12 (1973) 265–272.
[18] J.L. Atwood, F.R. Bennet, F.M. Elms, C. Jones, C.L. Raston, K.D. Robinson, J. Am. Chem. Soc. 113 (1991) 8183–8185.
[19] H. Vahrenkamp, Chem. Ber. 111 (1978) 3472–3483.